ELSEVIER

Journal of Organometallic Chemistry 514 (1996) 203–212

Journal of Organometallic Chemistry

Synthesis and characterization of triphenyl- and tri-n-butyltin pentafluorobenzoates, -phenylacetates and -cinnamates. X-ray structure determination of tri-n-butyltin pentafluorocinnamate

Rudolph Willem [a,b], Abdeslam Bouhdid [c], Monique Biesemans [a,b], José C. Martins [b], Dick de Vos [d], Edward R.T. Tiekink [e], Marcel Gielen [a,*]

[a] *Faculty of Applied Sciences, Laboratory for General and Organic Chemistry (AOSC), Room 8G512, Free University of Brussels (V.U.B.), Pleinlaan 2, B-1050 Brussels, Belgium*

[b] *High Resolution NMR Centre, Free University of Brussels (V.U.B.), Pleinlaan 2, B-1050 Brussels, Belgium*

[c] *Faculty of Sciences, Free University of Brussels (V.U.B.), Pleinlaan 2, B-1050 Brussels, Belgium*

[d] *Medical Department, Pharmachemie BV, NL-2003 RN Haarlem, Netherlands*

[e] *Department of Chemistry, The University of Adelaide, Adelaide, S.A. 5005, Australia*

Received 15 September 1995

Abstract

A crystal structure analysis of F_5C_6–CH = CH–$COOSnBu_3$ shows that the compound is polymeric because of the presence of bidentate carboxylate ligands bridging two tin atoms in *trans*-R_3SnO_2 arrangement. This results in a five-coordinated trigonal-bipyramidal geometry around the tin atom with two apical oxygen atoms and three equatorial butyl groups. Mössbauer and CP-MAS ^{117}Sn NMR data for triphenyl- and tri-n-butyltin pentafluorobenzoates, -phenylacetates and cinnamates, taking the X-ray structure of F_5C_6–CH=CH–$COOSnBu_3$ as a reference, converge to similar polymeric five-coordinated structures in the solid state. In contrast, ^{13}C and ^{119}Sn NMR data in chloroform solution unambiguously indicate tetrahedral four-coordination at tin for all compounds. Failing aromatic ^{13}C chemical shift increments and complex $^{n}J(^{13}C-^{19}F)$ multiplet patterns necessitated recording of 2D $^{19}F-^{13}C$ HMQC spectra in order to fully characterize the new compounds in solution.

Keywords: Tin; Fluorine; X-ray structure; NMR; Group 14

1. Introduction

The crystal structures of a number of triorganotin carboxylates have been determined by X-ray diffraction [1–3]. In the crystalline state, these compounds generally adopt either a polymeric structure with a five-coordinated tin atom (type A), or a monomeric one varying from a purely tetrahedral four-coordinated geometry (type C) to a similar one with a weak additional intramolecular coordination from the carbonyl oxygen to the tin atom (type B) [4–7] (see Fig. 1). An unusual cyclotetrameric structure has also been reported recently for tri-n-butyltin 2,6-difluorobenzoate [8].

The polymeric structure (A) is especially common in the crystalline state. However, sterically demanding groups apparently favour a monomeric structure (B or C). Furthermore, the electronegativity difference between the organic groups R and the carboxylate moiety also plays an important role [9]. Thus, a polymeric

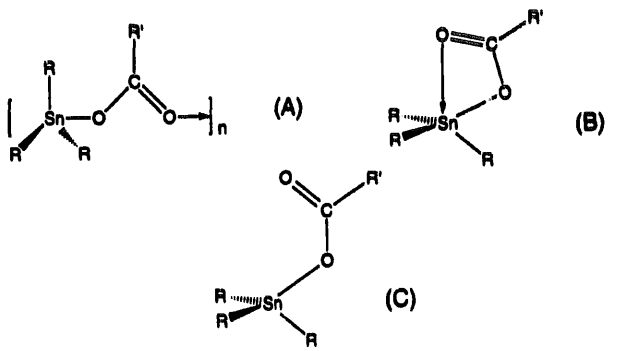

Fig. 1. Possible geometries for triorganotin carboxylates.

* Corresponding author.

SSDI 0022-328X(95)06040-5

structure (A) for tributyl- or -phenyltin carboxylates is associated with the R' group being electron withdrawing. The contribution of either steric or electronic factors has been discussed by Molloy et al. [7].

In general, triorganotin compounds display a higher biological activity than their di- and mono-organotin analogues. This has been attributed to their ability to bind to proteins [10–12]. Against human tumour cell lines, triphenyltin derivatives are highly active, being characterized by very low ID_{50} values [13].

We synthesized triphenyl- and tri-n-butyltin pentafluorobenzoates, -phenylacetates and -cinnamates (see Fig. 2) in order to find out which of them exhibits the expected polymeric structure. More precisely, we aimed at examining whether this is correlated with the electron withdrawing pentafluorophenyl group being directly or indirectly bound to the triorganostannyl carboxylate group. Only one of the compounds, F_5C_6–CH=CH–$COOSnBu_3$, provided suitable crystals for X-ray diffraction analysis. Its structure, combined with Mössbauer data and solid state ^{117}Sn CP-MAS NMR data for all compounds, enabled us to answer this question. Their in vitro antitumour activity was also screened.

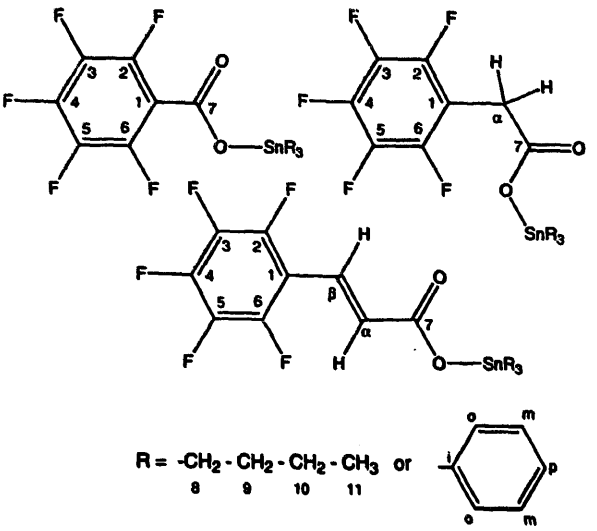

Fig. 2. Atom labelling scheme of the triphenyl- and tri-n-butyltin pentafluorobenzoates, -phenylacetates and -cinnamates.

2. Results and discussion

2.1. Syntheses

The new compounds synthesized obey the general formula F_5C_6–Z–CO_2SnR_3, where R = n-butyl or phenyl and Z is either absent or a CH_2 or CH=CH moiety. They were obtained by the condensation of the appropriate carboxylic acid with either tri-n-butyltin acetate [8,13,14] or triphenyltin hydroxide [7,15] in toluene/ethanol (4/1), and are listed in Table 1.

2.2. X-ray diffraction analysis of tri-n-butyltin pentafluorocinnamate

Suitable crystals of F_5C_6–CH=CH–$COOSnBu_3$ were obtained by recrystallization from a CH_2Cl_2/hexane solution. The crystallographic numbering scheme is shown in Fig. 3 and selected interatomic parameters are given in Table 2.

The structure conforms to the predominate motif found for triorganotin carboxylates, namely the polymeric five-coordinated *trans*-R_3SnO_2 geometry with two axial oxygen atoms and three equatorial R groups, as illustrated in Fig. 1(A). The Sn atom exists in a distorted trigonal bipyramidal environment with trigonal plane defined by the three butyl substituents. The axial positions are occupied by an O(1) atom and a symmetry related O(2)' atom (symmetry operation $0.5 - x$, $0.5 + y$, $-0.5 - z$), such that the diaxial angle is 169.71(9)°. The Sn atom lies 0.1557(3) Å out of the trigonal plane in the direction of the more strongly bound O(1) atom, i.e. Sn–O(1) is 2.201(3) Å and Sn–O(2)' is 2.413(3) Å. The disparity in the Sn–O distances is reflected in the associated C–O distances, the longer C–O bond involving the O(1) atom with the shorter Sn–O interaction. The polymeric structure, which is generated by the bidentate bridging carboxylate ligands, forms close F···F and F···H contacts to adjacent chains. The shortest non-hydrogen contact of 3.118(8) Å occurs between symmetry related F(6) atoms (symmetry relation $1 - x$, $-y$, $-z$). The carbon-backbone in the cin-

Table 1
Melting points, recrystallization solvents and yields for the triphenyltin and tributyltin pentafluorobenzoates, -phenylacetates and -cinnamates

Compound	M.p.(°C)	Recrystallization solvent	Yield (%)
$F_5C_6CO_2SnBu_3$	62–64	CH_2Cl_2/hexane	89
$F_5C_6CH_2CO_2SnBu_3$	79–80	CH_2Cl_2/hexane	83
$F_5C_6CH{=}CHCO_2SnBu_3$	71–73	CH_2Cl_2/hexane	89
$F_5C_6CO_2SnPh_3$	113–116	CCl_4	76
$F_5C_6CH_2CO_2SnPh_3$	135–137	CCl_4	73
$F_5C_6CH{=}CHCO_2SnPh_3$	108–111	CCl_4	75

Table 2
Selected interatomic bond distances (Å) and angles (°) for F_5C_6–CH=CH–$COOSnBu_3$

Sn–O(1)	2.201(3)	Sn–O(2)′	2.413(3)
Sn–C(11)	2.123(6)	Sn–C(21)	2.146(6)
Sn–C(31)	2.133(5)	O(1)–C(1)	1.278(5)
O(2)–C(1)	1.247(4)	C(1)–C(2)	1.480(5)
C(2)–C(3)	1.308(5)	C(3)–C(4)	1.457(6)
O(1)–Sn–O(2)′	169.71(9)	O(1)–Sn–C(11)	98.4(2)
O(1)–Sn–C(21)	96.2(2)	O(1)–Sn–C(31)	88.1(2)
O(2)′–Sn–C(11)	84.5(2)	O(2)′–Sn–C(21)	91.1(2)
O(2)′–Sn–C(31)	82.0(1)	C(11)–Sn–C(21)	118.1(2)
C(11)–Sn–C(31)	120.9(3)	C(21)–Sn–C(31)	119.5(3)
Sn–O(1)–C(1)	125.8(3)	Sn–O(2)′–C(1)′	143.5(3)
O(1)–C(1)–O(2)	122.9(4)	O(1)–C(1)–C(2)	116.8(4)
O(2)–C(1)–C(2)	120.3(4)	C(1)–C(2)–C(3)	122.9(4)
C(2)–C(3)–C(4)	128.7(4)		

Primed atoms are related by the symmetry operation $0.5 - x$, $0.5 + y$, $-0.5 - z$.

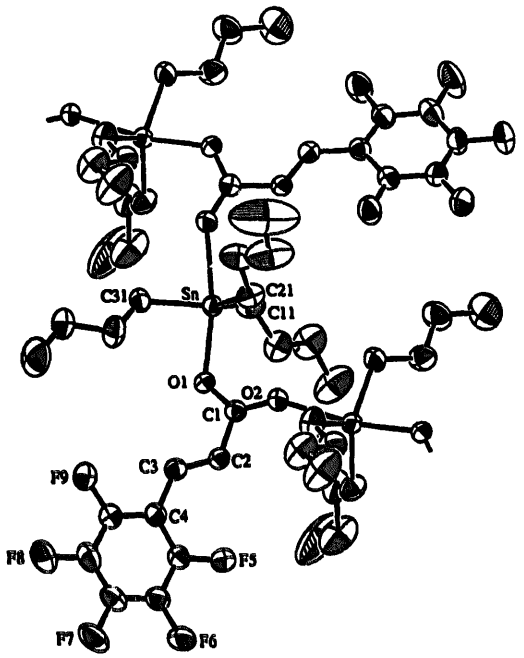

Fig. 3. Molecular structure and crystallographic numbering scheme for F_5C_6–CH=CH–$COOSnBu_3$.

namate ligand is essentially planar, as seen in the C(1)/C(2)/C(3)/C(4) torsion angle of −177.1(4)°; however, a slight twist is evident between this moiety and the carboxylate group [O(1)/C(1)/C(2)/C(3) is −13.4(7)°]; the dihedral angle between the planes through the C(1)–C(4) and C(4)–C(9) atoms is 12.2°.

The structure found here for F_5C_6–CH=CH–$COOSnBu_3$ may be compared with three other structurally characterized analogues in the literature [16]. The structural diversity observed in many organotin carboxylates [3] is found even in this limited sample. Analogous to F_5C_6–CH=CH–$COOSnBu_3$, polymeric structures, featuring *trans*-R_3SnO_2 geometries, are found in the structures of H_5C_6–CH=CH–$COOSnPh_3$ and *p*-Cl–H_4C_6–CH=CH–$COOSnPh_3$ [16], whereas a monomeric four-coordinated structure is observed for *p*-NO_2–H_4C_6–CH=CH–$COOSnPh_3$ [16]. It can be seen from the above that substituting a Cl for an NO_2 group results in a different structural motif despite the remoteness of this substitution from the tin centre.

2.3. ^{119}Sn Mössbauer data

The Mössbauer parameters of the $F_5C_6CO_2SnR_3$, $F_5C_6CH_2CO_2SnR_3$ and $F_5C_6CH{=}CHCO_2SnR_3$ compounds are listed in Table 3. The quadrupole splittings (QS) are found in the range 3.52–3.97 mm s^{-1}. Values of QS in the range 3.0–4.1 mm s^{-1} are typical for structures of type (A) [4,5,7,14] with a planar SnR_3 unit and two apical carboxylates. These observations ex-

Table 3
^{119}Sn Mössbauer parameters, QS (quadrupole splitting), IS (isomer shift relative to calcium stannate) and line widths (Γ_1 and Γ_2) for tributyl- and triphenyltin carboxylates, F_5C_6–Z–CO_2SnBu_3 and F_5C_6–Z–CO_2SnPh_3

Compound	IS	QS	Γ_1	Γ_2
F_5C_6–CO_2SnBu_3	1.53	3.97	0.93	0.98
F_5C_6–CH_2–CO_2SnBu_3	1.48	3.83	0.79	0.77
F_5C_6–CH=CH–CO_2SnBu_3	1.45	3.75	0.78	0.82
F_5C_6–CO_2SnPh_3	1.34	3.76	0.78	0.78
F_5C_6–CH_2–CO_2SnPh_3	1.31	3.55	0.87	0.87
F_5C_6–CH=CH–CO_2SnPh_3	1.31	3.52	0.76	0.76

Table 4
^{1}H NMR data in $CDCl_3$ for the F_5C_6-Z-CO_2SnBu_3 and F_5C_6-Z-CO_2SnPh_3 compounds; chemical shifts (ppm) with respect to TMS; coupling constants (Hz) in parentheses; d = doublet, m = complex pattern; s = singlet; t = triplet; tq = triplet of quartets; rough estimation of the unresolved $^3J(^1H-^{119/117}Sn)$ coupling constant for the *ortho* protons 120 ± 8 Hz

Compound	H-α of Z	H-β of Z	CH_2-α	CH_2-β	CH_2-γ	CH_3
F_5C_6-CO_2SnBu_3	—	—	m: 1.59–1.69	tq: 1.36 (7, 7)	tq: 1.35 (7, 7)	t: 0.90 (7)
F_5C_6-CH_2-CO_2SnBu_3	s: 3.67	—	m: 1.53–1.61	tq: 1.28 (7, 7)	tq: 1.25 (7, 7)	t: 0.88 (7)
F_5C_6-CH=CH-CO_2SnBu_3	d: 6.75 (16)	d: 7.52 (16)	m: 1.57–1.70	tq: 1.34 (7, 7)	tq: 1.30 (7, 7)	t: 0.91 (7)

Compound	H-α	H-β	H_o	H_{m-p}
F_5C_6-CO_2SnPh_3	—	—	m: 7.76–7.83	m: 7.47–7.54
F_5C_6-CH_2-CO_2SnPh_3	s: 3.82	—	m: 7.68–7.75	m: 7.44–7.51
F_5C_6-CH=CH-CO_2SnPh_3	d: 6.90 (16)	d: 7.70 (16)	m: 7.76–7.85	m: 7.44–7.53

clude structures of type B or C since such structures, proven by X-ray diffraction and with Mössbauer parameters determined [4,5,7], all displayed QS values in the range 2.36–2.97 mm s^{-1}, characteristic of monomeric structures with, however, no clear correlation to the length of the additional intramolecular coordination from the carbonyl oxygen to tin. Since the X-ray analysis provides evidence of a type A structure and the Mössbauer data are in agreement with such a structure for all compounds, it turns out that the electron withdrawing perfluorophenyl group, whether directly bound or not to the carboxylate group, favours polymer generation in the crystalline state. Further evidence for five-coordination is provided by ^{117}Sn CP-MAS NMR data (see below).

2.4. ^1H NMR data

The ^{1}H NMR data are shown in Table 4. The proton chemical shift assignment of the triorganotin moiety is straightforward from the multiplicity patterns and/or resonance intensities [17]. The assignment of the vinylic protons in the cinnamates required a $^{13}C-^1H$ HMQC experiment [18], establishing $^1J(^{13}C-^1H)$ correlations with the vinylic ^{13}C nuclei that were assigned from their $^nJ(^{13}C-^{19}F)$ multiplicity pattern (see below).

2.5. ^{19}F NMR data

The ^{19}F NMR data are presented in Table 5. The ^{19}F chemical shifts are in agreement with previous data on

Table 5
^{19}F NMR data in $CDCl_3$ for the F_5C_6-Z-CO_2SnBu_3 and F_5C_6-Z-CO_2SnPh_3 compounds; chemical shifts (ppm) with respect to external $CFCl_3$; coupling constants (Hz) in parentheses; dddd = doublet of doublets of doublets of doublets; bt = broad triplet

Compound	Fluorine	$\delta(^{19}F)$ (ppm)	$J(^{19}F,^{19}F)$ (Hz)
F_5C_6-CO_2SnBu_3	2 & 6	dddd: −140.2	[−21, 2, 2, +8]
	3 & 5	dddd: −162.0	[−21, −21, 3, +8]
	4	bt: −153.0	[−21]
F_5C_6-CH_2-CO_2SnBu_3	2 & 6	dddd: −143.5	[−21, 2, 2, +8]
	3 & 5	dddd: −163.9	[−21, −21, 2, +8]
	4	bt: −157.9	[−21]
F_5C_6-CH=CH-CO_2SnBu_3	2 & 6	dddd: −140.5	[−20, 2, 2, +8]
	3 & 5	dddd: −162.8	[−20, −20, 2, +8]
	4	bt: −153.5	[−20]
F_5C_6-CO_2SnPh_3	2 & 6	dddd: −138.3	[−19, 3, 1, +8]
	3 & 5	dddd: −161.9	[−19, −19, 3, +8]
	4	bt: −151.2	[−19]
F_5C_6-CH_2-CO_2SnPh_3	2 & 6	dddd: −142.5	[−21, 2, 2, +9]
	3 & 5	dddd: −162.9	[−21, −21, 3, +9]
	4	bt: −156.4	[−21]
F_5C_6-CH=CH-CO_2SnPh_3	2 & 6	dddd: −139.6	[−20, 2, 2, +8]
	3 & 5	dddd: −161.8	[−20, −20, 2, +8]
	4	bt: −151.9	[−20]

Table 6
^{13}C NMR data in $CDCl_3$ for the F_5C_6–Z–CO_2SnBu_3 compounds; chemical shifts (ppm) with respect to TMS; calculated aromatic chemical shifts in parentheses, $^nJ(^{13}C-^{19}F)$ coupling constants (Hz) bold, in braces; $^nJ(^{13}C-^{119/117}Sn)$ coupling constants in brackets (a single approximate value is given when the couplings with ^{119}Sn and ^{117}Sn are unresolved); bd = broad doublet; td = triplet of doublets. The aromatic ^{13}C chemical shifts, as well as the $^1J(^{13}C-^{19}F)$ coupling constants (±2 Hz), were deduced from the 2D $^{19}F-^{13}C$ HMQC spectra

Compound	F_5C_6–CO_2SnBu_3	F_5C_6–CH_2–CO_2SnBu_3	F_5C_6–CH=CH–CO_2SnBu_3
F_5C_6: C-1	td: 111.1 (101.8) {18; 4}	td: 110.1 (108.5) {19; 4}	td: 110.5 (107.9) {17; 4}
C-2≡C-6	bd: 144.7 (150.8) {263}	bd: 145.3 (149.9) {255}	bd: 145.4 (148.6) {262}
C-3≡C-5	bd: 137.5 (132.5) {268}	bd: 137.4 (134.4) {258}	bd: 137.7 (134.8) {259}
C-4	bd: 142.0 (134.1) {255}	bd: 140.0 (138.6) {255}	bd: 141.2 (141.8) {260}
C-α of Z	—	30.8	bs: 127.0
C-β of Z	—	—	bt: 128.7 {8}
CO	162.9	172.9	170.7
Sn–CH_2-α	17.1 [346/330]	16.7 [353/338]	16.6 [356/340]
CH_2-β	27.6 [22]	27.8 [20]	27.8 [20]
CH_2-γ	26.9 [63]	26.9 [64]	27.0 [64]
CH_3	13.5	13.5	13.5

organometallic compounds with a perfluorophenyl group [19,20]. The ^{19}F coupling patterns were elucidated by line shape simulation, using the data of Berger et al. [21] as starting trial values, with *ortho* $^3J(^{19}F-^{19}F)$ coupling constants being negative. Simulations were only satisfactory with positive $^5J(^{19}F-^{19}F)$ coupling constants. In contrast, the sign of the *meta* $^4J(^{19}F-^{19}F)$ coupling constants did not affect the line shapes which were, in general, broad ($\Delta\nu_{1/2} \approx 1-2$ Hz). Accordingly, the coupling constants are not reliable to better than 1 Hz.

The ^{19}F chemical shifts of the triphenyltin compounds are found systematically at higher frequencies than those of the tributyltin ones. This holds especially for the *ortho*-fluorine atoms of the benzoates. This observation is in agreement with the higher inductive electron withdrawing nature of the $SnPh_3$ group with respect to the $SnBu_3$ one.

2.6. ^{13}C NMR data

The ^{13}C NMR data are given in Tables 6 and 7. The assignment of the ^{13}C resonances of the aliphatic part is straightforward from the $^nJ(^{13}C-^{119/117}Sn)$ coupling constants. The aromatic resonances of the triphenyltin moieties are easily assigned on the basis of both aromatic $^nJ(^{13}C-^{119/117}Sn)$ coupling constants and signal intensities. The ^{13}C resonances of the C_6F_5 moieties are strongly dispersed, as a consequence of the multiple $^nJ(^{13}C-^{19}F)$ coupling splittings. Because the resonances are broad, the signal-to-noise ratio is low, accordingly the $^{13}C-^{19}F$ multiplets are ill defined and no attempt was made to determine the coupling constants $^nJ(^{13}C-^{19}F)$ ($n \geq 2$).

An initial trial assignment of the C_6F_5 ^{13}C resonances was achieved from aromatic chemical shift increments [22] determined for the $-COOSnR_3$, $-CH_2COOSnR_3$ and $-CH=CH-COOSnR_3$ (R = ^{n}Bu and Ph) from ^{13}C NMR spectra of the non-fluorinated analogues [23]. The agreement between experimental and calculated values is not satisfactory, especially for the *ortho* carbon atoms of the perfluorobenzoates and the pentafluorophenylacetates. This is attributed to the loss of incremental additivity related to the high degree of aromatic substitution. Accordingly, the assignments of Tables 6 and 7 were confirmed by a 2D HMQC $^{19}F-^{13}C$ correlation experiment [18] with ^{19}F detection. This was achieved according to the method recently proposed by Berger and coworker [24,25] using two NMR spectrometers. Details are given in the Experi-

Table 7
^{13}C NMR data in $CDCl_3$ for the F_5C_6–Z–CO_2SnPh_3 compounds; for further details see Table 6 caption

Compound	F_5C_6–CO_2SnPh_3	F_5C_6–CH_2–CO_2SnPh_3	F_5C_6–CH=CH–CO_2SnPh_3
C_6F_5: C-1	bs: 109.6 (101.2)	td: 109.5 (107.9) {18; 4}	td: 110.3 (107.6) {14; 4}
C-2≡C-6	bd: 145.5 (151.4) {266}	bd: 145.4 (149.9) {255}	bd: 145.7 (148.8) {261}
C-3≡C-5	bd: 137.6 (134.2) {268}	bd: 137.4 (134.5) {258}	bd: 137.7 (134.9) {266}
C-4	bd: 142.8 (144.8) {274}	bd: 140.6 (138.8) {268}	bd: 141.6 (142.2) {260}
CO	161.3	174.0	171.8
C-α of Z	—	28.1	bs: 128.8
C-β of Z	—	—	td: 127.3 {8, 2}
Sn–C_6H_5; C_i	137.1 [644/614]	137.5 [644/616]	138.1 [647/619]
C_o	136.9 [49/46]	136.8 [48]	136.9 [48]
C_m	129.2 [65/62]	129.6 [65/62]	129.1 [63]
C_p	130.7 [13]	130.5 [13]	130.1 [13]

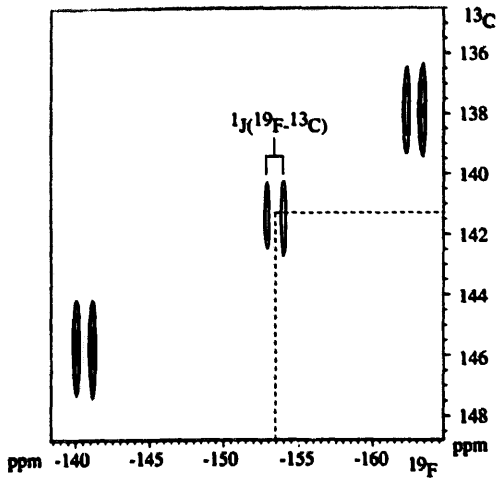

Fig. 4. Contour plot of the 2D ^{19}F–^{13}C HMQC spectrum in ^{19}F detection of F_5C_6-CH=CH-COOSnBu$_3$.

mental section. A typical contour plot is displayed in Fig. 4.

Holecek and coworkers [26–29] have shown that $^1J(^{13}C-^{119}Sn)$ coupling constants can be used to assess the coordination number of the tin atom in triorganotin compounds. Four-coordinated triphenyltin compounds exhibit couplings in the range 550–650 Hz, five-coordinated analogues in the range 750–850 Hz. Four-coordinated tributyltin compounds, however, exhibit couplings in the range 325–390 Hz, five-coordinated ones in the range 440–540 Hz.

All the triorganotin carboxylates of this investigation exhibit $^1J(^{13}C-^{119/117}Sn)$ coupling satellites in solution characteristic for tetrahedral compounds, the coupling constants being of the order of 350 Hz in the tributyltin compounds (Table 6) and 640 Hz in the triphenyltin ones (Table 7) [26,30]. The polymeric structure of the solid state is therefore lost in solution to generate a monomeric four-coordinated tetrahedral structure of type C.

The ^{13}C chemical shift of the *ipso*-carbon of the $SnPh_3$ moiety (see Table 7) around 138 ppm is also characteristic for a tetrahedral tin atom [31], since for five-coordinated triphenyltin carboxylates a value at approximately 4 ppm higher frequency is found. The $^1J(^{13}C-^{19}F)$ coupling constants of the di- and triorganotin pentafluorobenzoates lie in the usual range, 255–274 Hz, previously found for fluorobenzoates and aromatic fluorine compounds in general [8,17,32–34].

2.7. Tin NMR data

The ^{119}Sn NMR spectra of the tributyl- and triphenyltin compounds in $CDCl_3$ solution exhibit a single resonance in the range characteristic for tetrahedral compounds, between −83.3 and −104.3 ppm for the triphenyltin compounds and 118.7 and 148.0 ppm for the tributyltin compounds (see Table 8) [27]. This confirms the four-coordination proposed from the ^{13}C data. Indeed, for five-coordinated triphenyltin, respectively tributyltin compounds, the ^{119}Sn chemical shifts range from −180 to −280 ppm, respectively +40 to −60 ppm.

The ^{117}Sn CP-MAS NMR isotropic chemical shifts (see Table 8) obtained in the crystalline state are in agreement with five-coordination at tin as shown by the X-ray structure of tri-n-butyltin cinnamate. For the other compounds such ^{117}Sn chemical shifts, combined with the Mössbauer data which exclude the monomeric type B and C structures, strongly support the polymeric type A species. Thus, all data at hand indicate a loose polymeric structure with five-coordination at tin, that is lost in solution where a tetrahedral configuration is found. The splitting in the ^{117}Sn resonance observed in the solid state for the tri-n-butyltin perfluorobenzoate and pentafluorophenylacetate is assigned to slight non-equivalences of the structural moieties within the unit cell resulting from packing effects. In contrast, the splitting observed in triphenyltin perfluorobenzoate is larger and not readily explained by packing effects. Tentatively we propose this compound in the solid state to be polymorphous and to exist as two different five-coordinated structures which, upon dissolution, give rise to a single monomeric tetrahedral species. It is well established that polymeric or oligomeric organotin structures, present in the solid state and/or in concentrated solutions, can decompose to their monomers upon dilution [8,30].

A last point worth outlining is that the tin chemical shift towards lower frequency in the solid state with

Table 8
^{119}Sn NMR data in $CDCl_3$ and ^{117}Sn CP-MAS NMR data in the solid state for F_5C_6-Z-CO_2SnBu_3 and F_5C_6-Z-CO_2SnPh_3 compounds; chemical shifts (ppm), ($\Xi(^{119}Sn)$ = 37.290665 [36])

Compound	$\delta(^{119}Sn)(CDCl_3)$	$\delta(^{117}Sn)$(solid state)
F_5C_6-CO_2SnBu_3	148.0	38.2; 36.1
F_5C_6-CH_2-CO_2SnBu_3	127.2	−22.5; −25.2
F_5C_6-CH=CH-CO_2SnBu_3	118.7	−29.0
F_5C_6-CO_2SnPh_3	−83.3	−189.9; −216.1
F_5C_6-CH_2-CO_2SnPh_3	−96.0	−275.0
F_5C_6-CH=CH-CO_2SnPh_3	−104.3	−274.6

respect to the solution state is at least 40 ppm smaller for the perfluorobenzoates than for the pentafluorophenylacetates and pentafluorophenylcinnamates. This indicates the shielding of the tin nucleus, caused by the additional coordination, to be significantly smaller for the benzoates. We attribute this to the strong inductive electron withdrawing effect of the perfluorophenyl group being more effective in the benzoates than in the phenylacetates or cinnamates because it is closer to the carboxylate moiety in the former type of compounds. Accordingly, the tin–carboxylate interaction, leading to five-coordination, should be weaker, in agreement with the smaller shielding effect observed for the benzoates.

2.8. *In vitro antitumour screening*

The results of the in vitro antitumour screening of the six triorganotin fluorinated carboxylates against a selected panel of six human tumour cell lines: MCF-7 and EVSA-T, two breast tumours; WiDr, a colon carcinoma; IGROV, an ovarian cancer; M19 MEL, a melanoma; and A498, a renal cancer are presented in Table 9. The values of the previously synthesized tri-n-butyltin 2,6-difluorobenzoate [8], as well as clinically used reference compounds, are given for comparison [35].

The three tri-n-butyltin compounds are significantly more active or of the same order of activity against all cell lines when compared with the usual reference compounds [35]. The tri-n-butyltin pentafluorobenzoate is comparably or more cytotoxic when compared with its 2,6-difluoro analogue [8].

The triphenyltin pentafluorobenzoate and -cinnamate are less active than the tributyltin ones, but remain significantly more active than carboplatin, *cis*-platin and 5-fluorouracil. Surprisingly, triphenyltin pentafluorophenylacetate is more active than the tributyltin compounds against those cell lines, M19MEL and A498, where the latter derivatives display lowest activity.

3. Experimental

3.1. *Syntheses*

3.1.1. *Tri-n-butyltin compounds*

Equimolar quantities of tri-n-butyltin acetate and pentafluorobenzoic, pentafluorophenylacetic or pentafluorocinnamic acid were dissolved in a toluene/ethanol (4/1) mixture in a 250 ml flask equipped with a Dean-Stark funnel. This mixture was refluxed for 4 to 6 h. The ternary and subsequent binary azeotropes were distilled off, up to 50% of the initial solvent volume. The remaining solution was evaporated and the product obtained recrystallized from an appropriate solvent (see Table 1).

3.1.2. *Triphenyltin compounds*

Similarly an equimolar mixture of triphenyltin hydroxide and the suitable carboxylic acid were reacted and the desired compounds isolated and purified as above (see Table 1).

3.2. *Instrumental methods*

3.2.1. *Standard 1D and 2D NMR experiments*

All NMR spectra were recorded from $CDCl_3$ solutions or a Bruker AC250 spectrometer, using a QNP probe tuned at 250.13, 62.93, 93.28 and 235.36 MHz for ^{1}H, ^{13}C, ^{119}Sn and ^{19}F nuclei respectively. ^{1}H and ^{13}C resonances were referenced to the solvent peak at

Table 9
In vitro antitumour activities (ng ml^{-1}) against; MCF-7 and EVSA-T, two breast cancers; WiDr, a colon cancer; IGROV, an ovarian cancer; M19 MEL, a melanoma; and A498, a renal cancer, of tri-n-butyl- and triphenyltin pentafluorobenzoates, -phenylacetates and -cinnamates, together with those of some reference compounds used clinically and of tri-n-butyltin 2,6-difluorobenzoate

Compound	MCF-7	EVSA-T	WiDr	IGROV	M19 MEL	A498
F_5C_6–COOSnBu$_3$	15	< 3	20	25	60	50
F_5C_6–CH_2–COOSnBu$_3$	14	< 3	12	12	52	51
F_5C_6–CH=CH–COOSnBu$_3$	13	< 3	14	11	45	54
F_5C_6–COOSnPh$_3$	45	17	90	44	130	120
F_5C_6–CH_2–COOSnPh$_3$	14	6	17	20	18	30
F_5C_6–CH=CH–COOSnPh$_3$	20	9	30	34	40	37
2,6-$F_2H_3C_6$–COOSnBu$_3$ [8]	38	12	58	20	58	80
Carboplatin	10500	4500	3500	2400	5500	18000
Cis-platin	1400	920	1550	230	780	1200
5-Fluorouracil	350	720	440	850	310	340
Methotrexate	15	26	7	20	18	16
Doxorubicin	25	13	18	150	21	55

Table 10
Crystallographic data for F_5C_6-CH=CH-COOSnBu$_3$

Formula	$C_{21}H_{29}F_5O_2Sn$
Molecular weight	527.1
Crystal system	Monoclinic
Space group	$P2_1/c$
a (Å)	9.560(3)
b (Å)	10.679(2)
c (Å)	23.989(3)
β (°)	100.16(2)
V (Å^3)	2410.8(9)
Z	4
D_c (g cm^{-3})	1.452
F(000)	1064
μ (cm^{-1})	11.10
No. of data collected	6220
No. of unique data	5880
No. of reflections with $I \geq 3.0\sigma(I)$	3554
R	0.039
R_w	0.045
Residual ρ_{max} (e Å^{-3})	0.52

7.24 and 77.0 ppm respectively, while $\Xi(^{119}Sn) = 37.290665$ [36] was used for the ^{119}Sn resonances. ^{19}F resonances are referenced to $CFCl_3$ in $CDCl_3$.

The ^{19}F multiplicity patterns were simulated with the NMR" II 1.01 software from Calleo Scientific Software Publishers.

A proton-detected ^{1}H–^{13}C HMBC correlation spectrum was recorded on a Bruker AMX500 spectrometer interfaced with an X32 computer, using the standard program from the Bruker library [18].

3.2.2. 2D ^{19}F–^{13}C HMQC experiments [18,24,25]

2D ^{19}F{^{13}C} HMQC spectra were recorded by combining two NMR spectrometers in a single experiment as described by Berger and coworker [24,25]. All spectra were recorded on a Bruker AC 250 instrument at 310 K, on which the ^{19}F frequency was generated using samples in $CDCl_3$ with concentrations varying from 0.2 to 0.4 M.

The ^{13}C frequencies were generated on a Bruker AMX500 instrument. The QNP probe head on the AC250 spectrometer was tuned to ^{19}F on the proton channel and ^{13}C on the X channel. Spectra were recorded in 30 min with 1024 data points in F2 and 32 time increments in F1 using relaxation delays of 1 s and 48 scans for each FID. Prior to Fourier transformation, the data were zero filed to 256 points in F1. An exponential window in F2, with line broadening of 20 Hz, and a $\pi/2$ shifted square sine bell were used in F1.

3.2.3. CP-MAS ^{117}Sn spectra

All CP-MAS NMR spectra [37] were recorded on a Bruker AC250 spectrometer, operating at 89.15 MHz

Table 11
Fractional atomic coordinates for F_5C_6-CH=CH-COOSnBu$_3$

Atom	x	y	z
Sn	0.28426(3)	0.77546(3)	−0.22679(1)
F(5)	0.4571(4)	0.2059(3)	−0.0588(1)
F(6)	0.6317(5)	0.0835(3)	0.0223(1)
F(7)	0.8581(4)	0.1981(4)	0.0827(1)
F(8)	0.9087(4)	0.4421(4)	0.0624(2)
F(9)	0.7359(4)	0.5674(3)	−0.0189(1)
O(1)	0.3398(3)	0.6262(2)	−0.1635(1)
O(2)	0.2586(3)	0.4641(3)	−0.2174(1)
C(1)	0.3291(5)	0.5086(4)	−0.1732(2)
C(2)	0.4064(5)	0.4248(4)	−0.1291(2)
C(3)	0.5034(5)	0.4650(4)	−0.0876(2)
C(4)	0.5915(5)	0.3930(5)	−0.0431(2)
C(5)	0.5688(6)	0.2678(5)	−0.0305(2)
C(6)	0.6584(7)	0.2029(5)	0.0115(2)
C(7)	0.7707(7)	0.2612(6)	0.0426(2)
C(8)	0.7976(6)	0.3838(7)	0.0321(2)
C(9)	0.7068(6)	0.4477(5)	−0.0100(2)
C(11)	0.0612(6)	0.7775(6)	−0.2293(3)
C(12)	−0.0114(6)	0.6658(6)	−0.2125(3)
C(13)	−0.1694(7)	0.6650(9)	−0.2222(4)
C(14)	−0.2388(8)	0.5566(8)	−0.2013(5)
C(21)	0.3637(6)	0.6821(5)	−0.2940(2)
C(22)	0.4481(8)	0.7522(6)	−0.3280(3)
C(23)	0.4928(11)	0.6724(8)	−0.3744(4)
C(24)	0.5564(23)	0.7302(12)	−0.4109(7)
C(31)	0.4209(7)	0.8973(5)	−0.1714(2)
C(32)	0.5568(6)	0.8459(6)	−0.1403(3)
C(33)	0.6616(7)	0.9339(6)	−0.1079(3)
C(34)	0.7854(8)	0.8825(9)	−0.0721(4)

for the ^{117}Sn nucleus. The spectrometer is interfaced with an Aspect 3000 computer and equipped with an MAS broad-band probe for solid state experiments. The matching condition for Hartmann–Hahn cross-polarization [37] (^1H 90°, pulse length 5 ms) was set with $(C_6H_{11})_4Sn$ for the ^{117}Sn nucleus [38] as well as the chemical shift reference [−97.35 ppm relative to $(CH_3)_4Sn$]. 7 mm outside diameter ZrO_2 rotors were used. The ^{117}Sn spectra were typically obtained by acquiring 32K data points over a spectral width of 166.7 kHz, a 2 ms contact time and a relaxation delay of 2 s with 1000 to 10000 scans. In order to find the isotropic ^{117}Sn chemical shift, spectra were run at two or three different spinning rates [37].

^{117}Sn spectra were recorded instead of the more common ^{119}Sn ones in order to overcome a local radio interference problem [39,40]. $^{117}Sn/^{119}Sn$ isotopic effects on tin chemical shifts are known to be negligible [41].

3.2.4. X-ray crystallography

Intensity data for a colourless crystal (0.13 × 0.19 × 0.36 mm^3) were measured at room temperature on a Rigaku AFC6R diffractometer fitted with Mo Kα radiation (graphite monochromator, $\lambda = 0.71073$ Å) employing the $\omega/2\theta$ scan technique up to θ_{max} 27.5°. No decomposition of the crystal occurred during the data collection, the data were corrected for Lorentz and polarization effects [42] and for absorption employing an empirical procedure [43]. Crystal data are summarised in Table 10. The structure was solved by direct methods [44] and refined by a full-matrix least-squares procedure based on F [42]. Non-hydrogen atoms were refined with anisotropic thermal parameters and hydrogen atoms were included in the model at their calculated positions (C–H 0.97 Å). Though high thermal motion was found for the butyl chain C(21)–C(24), only one position was detected for each atom; final refinement details (sigma weights) are collected in Table 10. Final fractional atomic coordinates for the non-hydrogen atoms are listed in Table 11 and the numbering scheme employed is shown in Fig. 3, which was drawn with ORTEP at 30% probability ellipsoids [45]. Data manipulation was performed with the TEXSAN program [42] installed on an Iris Indigo work station. Other crystallographic details, comprising thermal parameters, H-atom parameters, all bond distances and angles and tables of observed and calculated structure factors, are available on request (E.R.T.T.).

3.2.5. Mössbauer spectroscopy

Mössbauer spectra were obtained as described previously [46].

3.2.6. In vitro screening

The in vitro tests were performed as described previously [35].

Acknowledgments

We thank Mrs. I. Verbruggen for recording the NMR spectra. We are grateful to Mr. H.J. Kolker, Dr. J. Verweij, Professor Dr. G. Stoter and Dr. J.H.M. Schellens, Laboratory of Experimental Chemotherapy and Pharmacology, Department of Medical Oncology, Rotterdam Cancer Institute, NL-3008 AE, Rotterdam, Netherlands, for performing the in vitro tests. We thank Professor Dr. B. Mahieu for recording the Mössbauer spectra. This research was supported by the Belgian Nationaal Fonds voor Wetenschappelijk Onderzoek (NFWO, Grant No. S2/5 CD F198, M.G.), the Belgian Fonds voor Kollektief Fundamenteel Onderzoek (FKFO, Grant No. 2.0094.94, R.W., M.B.), the Belgian Nationale Loterij (Grant No. 9.0006.93, R.W., M.B.), the Human Capital and Mobility Programme of the European Community (Contract No. ERBCHRXCT920016) and the Australian Research Council (crystallographic facility). Professor Dr. S. Berger, Universität Marburg, Germany, is gratefully thanked for providing information prior to publication on ^{13}C, ^{19}F correlations as well as for useful suggestions.

References

[1] S.W. Ng, V.G. Kumar Das, F. Van Meurs, J.D. Schagen and L.H. Straver, *Acta Crystallogr., C, 45* (1989) 570.
[2] E.R.T. Tiekink, G.K. Sandhu and S.P. Verma., *Acta Crystallogr., C, 45* (1989) 1810.
[3] E.R.T. Tiekink, *Appl. Organomet. Chem., 5* (1991) 1.
[4] R.R. Holmes, R.O. Day, V. Chandrasekhar, J.F. Vollano and J.M. Holmes, *Inorg. Chem., 25* (1986) 2490.
[5] P.J. Smith, R.O. Day, V. Chandrasekhar and J.M. Holmes, *Inorg. Chem., 25* (1986) 2495.
[6] K.C. Molloy, T.G. Purcell, M.F. Mallon and E. Minshall, *Appl. Organomet. Chem., 1* (1987) 507.
[7] K.C. Molloy, S.J. Blunden and R. Hill, *J. Chem. Soc., Dalton Trans.*, (1988) 1259.
[8] M. Gielen, A. El Khloufi, M. Biesemans, F. Kayser, R. Willem, B. Mahieu, D. Maes, J.N. Lisgarten, L. Wyns, A. Moreira, T.K. Chattopadhay and R. Palmer, *Organometallics, 13* (1994) 2849.
[9] R.G. Vollano, R.O. Day, D.N. Rau, V. Chandrasekhar and R.R. Holmes, *Inorg. Chem., 23* (1984) 3153.
[10] A.G. Davies and P.J. Smith, *Adv. Inorg. Chem. Radiochem., 1* (1980) 23.
[11] W.N. Aldridge, in J.J. Zuckerman (ed.), *Organotin Compounds. New Chemistry and Applications*, Adv. Chem. Ser., Vol. 168, Am. Chem. Soc., Washington, 1976, p. 157.
[12] B.M. Elliot, W.N. Aldridge and J.M. Bridges, *Biochem. J., 177* (1979) 461.
[13] R.C. Poller, *The Chemistry of Organotin Compounds*, Academic Press, New York, 1970.
[14] A.G. Davies and P.J. Smith, in G. Wilkinson (ed.), *Comprehensive Organometallic Chemistry*, Pergamon Press, Oxford, 1982, Chapter 11, p. 564.
[15] K.C. Molloy, K. Quill, S.J. Blunden and R. Hill, *Polyhedron, 5* (1986) 959.
[16] S.L. Foong, S.W. Ng, M. Gielen and V.G. Kumar Das, *Malaysian J. Sci., 15B* (1994) 13.

[17] E.R.T. Tiekink, M. Gielen, A. Bouhdid, M. Biesemans and R. Willem, *J. Organomet. Chem.*, *494* (1995) 247.
[18] A. Bax, R.H. Griffey and B.H. Hawkins, *J. Magn. Reson.*, *55* (1983) 301.
[19] K. Ludovici, W. Ryrra and D. Naumann, *J. Organomet. Chem.*, *444* (1992) 363.
[20] W.A. Wan Abu Bakar, J.L. Davidson, E. Lindsell and K.J. McCullough, *J. Chem. Soc., Dalton Trans.* (1990) 61.
[21] S. Berger, S. Braun and H.O. Kalinowski, *NMR-Spektroskopie von Nicht-Metallen, Band 4, ^{19}F NMR Spectroscopy*, Thieme Verlag, Stuttgart, 1994.
[22] H.O. Kalinowski, S. Berger and S. Braun, *Carbon NMR Spectroscopy*, Wiley, Chichester, UK, 1988, p. 313.
[23] M. Gielen, A. Bouhdid, M. Biesemans and R. Willem, unpublished results.
[24] S. Berger, *J. Fluorine Chem.*, *72* (1995) 117.
[25] S. Berger and N. Wetzel, *TAMU-NMR Newsletter*, 12 (April 1994).
[26] J. Holecek, M. Nadvornik, K. Handlir and A. Lycka, *J. Organomet. Chem.*, *241* (1983) 177.
[27] M. Nadvornik, J. Holecek, K. Handlir and A. Lycka, *J. Organomet. Chem.*, *275* (1984) 43.
[28] A. Lycka, J. Holecek, M. Nadvornik and K. Hadler, *J. Organomet. Chem.*, *280* (1985) 323.
[29] J. Holecek, K. Handlir, M. Nadvornik and A. Lycka, *J. Organomet. Chem.*, *258* (1983) 147.
[30] I. Omae, *J. Organomet. Chem. Lib.*, *21* (1939) 95.
[31] A. Lycka, M. Nadvornik, K. Handlir and J. Holecek, *Collect. Czech. Chem. Commun.*, *49* (1984) 2903.
[32] H.O. Kalinowski, S. Berger and S. Braun, *Carbon NMR Spectroscopy*, Wiley, Chichester, UK, 1988, p. 579.
[33] M. Gielen, E.R.T. Tiekink, A. Bouhdid, D. de Vos, M. Biesemans, I. Verbruggen and R. Willem, *Appl. Organomet. Chem.*, *9* (1995) 639.
[34] M. Gielen, M. Biesemans, A. El Khloufi, J. Meunier-Piret, F. Kayser and R. Willem, *J. Fluorine Chem.*, *64* (1993) 279.
[35] Y.P. Keepers, P.E. Pizao, G.J. Peters, J. Van Ark-Otte, B. Winograd and H.M. Pinedo, *Eur. J. Cancer*, *27* (1991) 897.
[36] J. Mason, *Multinuclear NMR*, Plenum Press, New York, 1987, p. 627.
[37] F.A. Bovey, L. Jelinski and P.A. Mirau, *Nuclear Magnetic Resonance Spectroscopy*, Academic Press, San Diego, 2nd Edn., 1987, Chapter 8, pp. 399–434.
[38] A. Sebald, MAS and CP/MAS NMR of Less Common Spin-1/2 Nuclei, in P. Diehl, E. Fluck, H. Günther, R. Kosfeld and J. Seelig (eds.), *Solid State NMR II: Inorganic Matter*, Springer, Berlin, 1994; p. 91.
[39] B.R. Koch, G.V. Fazakerley and E. Dijkstra, *Inorg. Chim. Acta*, *45* (1980) L51.
[40] P.G. Harrison, in P.G. Harrison, (ed.), *Chemistry of Tin*, Blackie, Glasgow, 1989, Chapter 3, p. 113.
[41] H.C.E. McFarlane, W. McFarlane and C.J. Turner, *Mol. Phys.*, *37* (1979) 1639.
[42] *TEXSAN, Crystal Structure Analysis Package*, Molecular Structure Corp., TX, 1992.
[43] N. Walker and D. Stuart, *Acta Crystallogr., A39* (1983) 158.
[44] G.M. Sheldrick, *SHELXS86, Program for the automatic solution of crystal structure*, University of Göttingen, Germany, 1986.
[45] C.K. Johnson, *ORTEPII*, Rep. 5136, Oak Ridge National Laboratory, TN, 1976.
[46] R. Willem, A. Delmotte, I. De Borger, M. Biesemans, M. Gielen and F. Kayser, *J. Organomet. Chem.*, *480* (1994) 255.